Energy Advances

ROYAL SOCIETY OF CHEMISTRY

PAPER

View Article Online
View Journal | View Issue

Cite this: *Energy Adv.*, 2026, 5, 696

An integrated pyrolysis approach for hydrogen production and microplastic elimination from sewage sludge: experimental and analytical perspectives

Charles Wilde, Kumar Vijayalakshmi Shivaprasad, * Abdullah Malik, Yaodong Wang, Anthony Paul Roskilly and Huashan Bao

Municipal sewage sludge, a byproduct of wastewater treatment processes, is increasingly recognised as a reservoir of microplastics (MP), posing environmental risks to soil and water systems. This study evaluates pyrolysis as an integrated solution for recovering hydrogen-rich syngas and eliminating MPs from sewage sludge. The sludge, sourced from a wastewater treatment facility in the United Kingdom, was pre-treated through conditioning and drying before being thermochemically converted at 800 °C. Varying the auger speed revealed that slower speeds significantly improved hydrogen output, reaching up to 41 vol%, primarily due to extended gas residence time that favours secondary reforming and cracking reactions. Quantitative analysis of MPs showed a significant reduction, from an initial concentration of 53.7 ± 7.2 MPs per g in dried sludge to undetectable levels in the resulting biochar. Morphological characterization identified fragments (46.2%) and fibres (41.9%) as dominant MP types, with further evaluation of their size and colour profiles. FTIR spectroscopy confirmed the presence of polyethylene terephthalate (PET) in untreated sludge and the absence of plastic-related signals in post-pyrolysis samples. The results highlight pyrolysis as a promising method for concurrent clean energy recovery and microplastic remediation, offering practical guidance for advancing circular economy goals and sustainable waste-to-hydrogen pathways.

Received 11th August 2025,
Accepted 28th February 2026

DOI: 10.1039/d5ya00228a

rsc.li/energy-advances

1. Introduction

1.1 Microplastics: sources and growing environmental concerns

The growing dependence on fossil fuels has intensified global energy security challenges and significantly contributed to environmental degradation. In the search for sustainable alternatives, biomass has attracted considerable attention due to its renewability and potential for carbon-neutral energy generation. As of September 2024, bioenergy contributes 6.6% to the United Kingdom's renewable energy portfolio, supplying over 43% of the nation's total energy from renewable sources. In alignment with climate policy goals, the UK has pledged to reach net-zero greenhouse gas emissions by 2050.[1] One pathway supporting this transition is the conversion of biomass into hydrogen-rich syngas, which holds promise for both energy recovery and carbon emission reduction. Within this context, hydrogen (H_2) has emerged as a clean energy vector with significant potential for integration into low-carbon energy systems.

Pyrolysis, a thermochemical transformation process operating under limited oxygen, has been extensively studied for its ability to convert the organic content of sewage sludge (SS) into valuable by-products such as biochar, bio-oil, and syngas.[2] This process offers an efficient route for carbon redistribution while minimizing waste volume. Among the products, biochar is especially notable due to its high carbon content and porous structure, which make it suitable for applications in environmental remediation, catalysis, and soil enhancement.[3] Additionally, pyrolysis facilitates the stabilization of inorganic pollutants, effectively reducing their mobility and environmental hazards. The liquid and gaseous outputs of pyrolysis also offer significant value. Bio-oil can be used as a renewable fuel or converted into industrial chemicals, whereas syngas, primarily composed of hydrogen, carbon monoxide, and methane, is a versatile energy carrier and feedstock for chemical synthesis.[4]

Recent innovations in reactor design have made pyrolysis more viable for sewage sludge treatment. For example, a twin-auger pyrolysis reactor specifically for sludge processing,

Department of Engineering, Durham University, Durham, DH1 3LE, UK.
E-mail: shivaprasad.k.vijayalakshmi@durham.ac.uk

reporting product yields of 50% bio-oil, 40% syngas, and 10% biochar at 500 °C.[5] Similarly, co-pyrolysis, which involves blending sewage sludge with other feedstocks, has shown enhanced energy recovery potential. Combining sewage sludge with rice husk, which resulted in a 41.55% increase in syngas energy content, improving the lower heating value (LHV) from 7.99 MJ N^{-1} m^{-3} to 11.31 MJ N^{-1} m^{-3} through synergistic effects and optimised process conditions.[6]

While pyrolysis presents a promising route for energy generation and waste minimization, current practices for managing sewage sludge primarily involve biological treatments like anaerobic digestion or chemical stabilization with agents such as lime.[7] The treated sludge is frequently applied to agricultural land as a nutrient source. However, sewage sludge also serves as a reservoir for a wide array of contaminants, including organic and inorganic microplastics (MP), pathogens, heavy metals, and chemical residues.[8] When applied to soil, these pollutants can enter the terrestrial ecosystem, where microplastics pose emerging environmental and health risks. Due to their resilience and transportability, MPs may serve as carriers for harmful substances and pathogens, potentially impacting soil health, disrupting ecosystems, and accumulating in the food chain over time.

Microplastics are defined by the U.S. National Oceanic and Atmospheric Administration and the European Chemicals Agency as plastic particles less than 5 mm in length.[9,10] The term ''microplastic'' was first coined by Professor Richard Thompson in 2004 and the research into their detrimental environmental impact has accelerated.[11] Recent studies highlight that MPs have infiltrated into every environment from Arctic Sea ice to human blood.[12,13] Waste water treatment plants (WWTPs) have been identified as a major sink for domestic MPs,[14] with concentrations as high as 3.14×10^4 particles per L entering individual WWTPs.[15] Of these, 69–80% are transferred to sludge.[16] From WWTPs, the MP's contaminated sludge is transferred to agricultural environments, where their adverse effects on crop and soil health are beginning to be recognised.[17,18] Therefore, the quantification and analysis of MP morphologies (type, shape, size) in biochar can provide valuable insight into the impact of MPs dumping on soil and plant health, and ultimately their potential environmental risks.

Over the past five years, there has been growing focus on analysing MP concentrations in raw sewage. However, many studies explain the current shortfalls in the standardization of methods, which makes the results hard to compare and cross-reference.[19,20] There is also a pressing need to develop technologies that can effectively reduce MPs in sewage sludge. Pyrolysis has been proven an effective treatment method for removing MPs, along with other contaminants such as pathogens and organic pollutants.[21,22] This process involves heating organic material in the absence of oxygen to high temperatures to carbonise the material and produce syngas, as well as bio-oils, which are promising alternative energy sources in the decarbonization of the power, transport, and the heating sectors.[23] However, as this process is relatively novel in WWTPs, more research is required to determine the optimal pyrolysis conditions for effective degradation of sludge and production of biochar, syngas, and bio-oils.

The MPs in sludge can be classified into two group: primary and secondary MPs.[24] Primary MPs are specially manufactured microplastics such as fragments and microbeads, commonly found in cleaning agents and personal care products. The properties that make plastics so useful, such as lightweight and slow decay/breakdown, also characterise their environmental polluting potential. The release of primary MPs can greatly reduce by government legislation and policies, enforcing a transition away from MP products. Secondary MPs consist of smaller fragments of plastic that originate from the breakdown of larger plastic items. These include synthetic fibres from washing clothes, erosion of everyday plastic items, and rubber tyre particles.[25] Actions to reduce secondary MP pollution may involve the development of novel materials engineered to shed fewer particles. However, in the modern and consumer driven world, a transition from plastics to more expensive, eco-friendly materials is likely to be a slow and gradual process.

MPs ranging between 1 and 100 nm in size are often referred to as nano plastics (NPs). Like MPs, NPs can be classified into primary and secondary forms. However, their effect on human health is of great concern as they are small enough to enter the blood stream *via* the respiratory system causing inflammation, physical stress, and immune responses. This research does not focus on NPs as their detection is very resource intense, however, there is great potential for further studies into their impacts on soil and plant health.[13] As MPs have infiltrated almost every corner of the earth, their impact is being observed in many environments.[12,13] Numerous studies have highlighted MP's effects in marine environments, referring to their impact on the terrestrial environments of soil and crops.[26,27] The use of sludge in agricultural varies largely between countries but in the UK, around 87% (3.5 million tonnes) of sewage sludge was recycled onto agricultural land in 2020.[28] The main treatment methods for this sludge are anaerobic digestion and lime stabilization. However, within these treatment methods there is ongoing debate over the rates of salmonella, toxic chemicals, and plastic present in sewage sludge used on farmland.[29]

Previous studies have estimated that the concentration of MPs in UK soil ranges from 1320 to 8190 particles per kg of soil.[30] It is believed, due to a mix of slurry, waterways, irrigation, plastic-coated fertilisers, and agricultural waste, that agricultural soils contain the highest MP concentration of any environment worldwide.[31] The effect of MPs on the soil and plant health is an emerging area of study within the MP field. MPs are known for disrupting soil structure and adversely impacting its porosity. If MPs are accumulated in high concentration, they can block soil pores and disrupt the soil's infiltration capacity. This can alter the soil structure, disturb the nutrient cycle, and affect crop growth.[18] MPs have the potential to act as carriers for chemical pollutants within the soil matrix. Potentially toxic elements (PTEs), harmful to the environment can be absorbed by MPs due to their rough, large surface areas and under certain conditions, release them into the soil structure.[17] The detrimental effect of MPs in the terrestrial

environment also stretches to decreased enzymatic activity, lower microbial diversity, and decreased plant growth. Despite previous studies, it is important to acknowledge that the research into MPs' effects on soil health is still in its infancy, as research only began ten years ago. As more research is conducted, our understanding into the harmful extent of MPs will continue to grow.

1.2 Microplastics: pre-treatment methods and analysis techniques

Samples of biochar and dried, raw sludge are to be treated prior to any identification and quantification of MPs. Organic matter, sediments and metals must be removed from samples to grant clear visual and chemical analysis of their MP composition. In particular, organic matter has a density similar to that of MPs, which can significantly error in MP quantification when using visual microscopy.[20] Therefore, removal of organic matter is the first essential step in the preparation process. While advanced techniques such as thermal decomposition and pressurised liquid extraction exist,[32,33] they are costly, time consuming, and require specialised equipment. Previous studies illustrate the use of hydrogen peroxide (H_2O_2),[20] enzymes (protease, lipase and cellulase)[19] and Fenton's reagent to remove organic matter. Fenton's reagent is an oxidation process utilizing H_2O_2 in the presence of an Fe^{2+} catalyst. Due to its simplicity, this study assessed the extent of organic matter removal *via* simple peroxide oxidation.[22]

The density separation method has been employed to remove inorganic substances from the biomass sample. A zinc chloride is commonly used solution for this purpose,[20] because it is more effective at separating heavier plastics than other solutions, such as sodium chloride or magnesium chloride, due to its higher density.[34] However, zinc chloride is more expensive and requires specialized disposal due to hazardous nature. To reduce intense resource utilization, this study used a saturated sodium chloride solution.

The first stage of MP quantification is visual identification through microscopic analysis. Manually sorting plastics particles under a microscope is most effective for particles >500 μm.[25] Visual identification is a commonly used preliminary method for MP identification and quantification, but it is prone to inaccuracies. Optical microscopy is much faster for evaluating larger samples for MP quantity than relying solely on spectroscopy techniques. To avoid misidentification and overestimation of MPs, it is important to standardise a plastic particle selection procedure.[20] Some studies recommend heating the samples in what is known as a 'hot needle test' to identify the melted polymers more easily,[35] while others use polarised light microscopy in which certain synthetic particles appear vibrantly illuminated. Zubris and Richards implemented a pre-treatment stage to eliminate the majority of non-microplastic constituents. In addition to visual identification, representative subsamples of suspected plastic particles were subjected to chemical analysis to quantify the reliability of visual discrimination.[36] In existing literature, scanning electron microscopy (SEM) is often used to analyse morphology of MPs. It has been highlighted that surface roughness has a direct correlation with potential toxic element (PTE) absorption. These PTEs are then released further into the soil matrix and research shows that MPs can even carry these pollutants into organisms. SEM can display the MP surface degradation and cracks whilst also revealing smaller microplastics, in the order of 10 nm.[26,37]

MPs are synthetic polymers composed of a wide range of chemical compounds with different chemical properties. Spectroscopy techniques can provide the number, size, and chemical composition of MPs rather than the total mass of plastics. Typically, only a fraction of the identified particles in a sample are analysed and extrapolated to obtain the overall plastic content.[14] Hence, these techniques make assumptions based on sub-samples to save time. Novel, direct mass measuring techniques exist, such as mass spectrometry alongside pyrolysis-gas chromatography,[38] or thermogravimetric analysis coupled with differential scanning calorimetry.[39] However, these techniques are destructive as they breakdown the MPs during their analysis and prevent shape and colour determination.

Alongside the morphology inspection in this study, non-destructive techniques such as Fourier transform infrared spectroscopy (FT-IR) and Raman spectroscopy can be used. Raman spectroscopy is based upon the interaction of light with the chemical bonds in a material process returns a transmittance vs wavenumber spectrum where the peaks relate to specific chemical bonds present in a material. These can be compared to the signature peaks of bonds in a spectra table to identify the composition of a given MP.[40] Critical comparisons from previous papers highlight the advantages and disadvantages of either method. It is explained that bands that have strong Raman intensities can in many cases have weak IR intensities and *vice versa*. Hence, an ideal analysis would utilise both methods, however, this is very time consuming so only one method is used in this study. Raman analysis has been shown to have better size resolution (down to 1 μm) whilst FTIR can only detect particles to a size of 10–20 μm.[41] Studies have also shown that Raman spectroscopy identifies up to 100% more 10–500 μm MPs in each sample when compared to FTIR spectroscopy but requires a four-times higher analysis time.[42]

1.3 Novelty and significance of the study

This study presents a novel dual-function pyrolysis strategy that, for the first time, achieves both high-yield hydrogen-rich syngas production and microplastic removal from real municipal sewage sludge. In contrast to previous studies that address energy recovery or pollutant remediation separately, this work integrates both outcomes within a single thermochemical process. The research characterises and quantifies the syngas composition, as well as the occurrence and types of MPs, in both untreated sludge and pyrolysed biochar. It further assesses the efficiency of MP removal at operating pyrolysis temperatures and critically reviews existing MP analytical methods, proposing recommendations towards a standardised protocol for application across the wastewater treatment sector.

Overall, the findings demonstrate a scalable and practical pathway for coupling waste-to-hydrogen conversion with effective MP remediation, contributing to circular economy objectives and advancing environmental protection strategies beyond the scope of earlier single-focus studies.

2. Methodology

2.1 Sludge drying and pyrolysis

Ongoing research continues to explore the potential of sewage sludge as a viable biomass resource for fuel production. The moisture content of raw sludge, typically ranging between 40% and 90%, varies depending on the treatment methods employed at wastewater facilities. However, effective sludge conversion through thermochemical processes such as pyrolysis requires the feedstock to be sufficiently dried in advance.

Sludge drying is not merely a preparatory step but a critical component that should be integrated into the overall thermal treatment strategy. Compared to even the most advanced mechanical dewatering methods, thermal drying offers significantly improved moisture reduction, making it more suitable for energy recovery applications. As illustrated in Fig. 1, the wet sludge in this study was dried using a tumble dryer until a residual moisture content of approximately 15% was achieved. This drying process yielded around 300 grams of dry sludge per kilogram of wet input. The dried sludge was then subjected to proximate and ultimate analyses, the results of which are summarised in Table 1, to characterise its composition and assess its suitability as a pyrolysis feedstock.

Subsequent pyrolysis experiments were conducted using a commercially available pyrolyser system, shown in Fig. 1, manufactured by Hybrid Gasification Limited. This system consists of a material feeder, heating chamber, biochar collector, gas filtration setup, and a gas analysis module. For each experimental run, 500 grams of dried sludge were fed into the pyrolysis chamber. The process was carried out at a temperature of 800 °C, which enabled efficient syngas production. After pyrolysis, the solid residue biochar was collected and retained for detailed microplastic analysis. The composition of the produced syngas, including hydrogen (H_2), carbon monoxide (CO), carbon dioxide (CO_2), methane (CH_4), ethylene (C_2H_4), and light hydrocarbons collectively reported as C_nH_m, was measured using a Cubic Instruments Gasboard-3100 infrared syngas analyser. Reproducibility was assessed by repeating key experiments under identical conditions, with observed variations in syngas composition and flow rate falling within acceptable experimental uncertainty associated with the measurement methods.

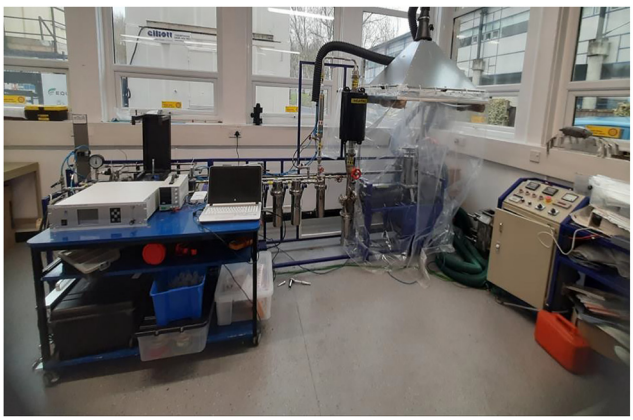

Fig. 1 Photographic view of 1 kg h^{-1} capacity of pyrolyser.

Table 1 Ultimate and proximate analyses of biomass

Proximate analysis			
	Moisture content	wt%	15
	Ash content	wt%	25.4
	Volatile matter	wt%	51.3
	Fixed carbon	wt%	8.3
Ultimate analysis			
	Carbon	wt%	30.06
	Hydrogen	wt%	4.68
	Nitrogen	wt%	4.38
	Sulphur	wt%	1.65

The elemental composition of the pyrolytic char as tabulated in Table 2 was assessed using a handheld Niton XL3t portable X-ray fluorescence (pXRF) spectrometer. The analysis was performed in the 'Mining Cu/Zn' mode, which is specifically calibrated to detect a range of metallic and mineral elements commonly found in thermochemically treated biomass residues. This approach enabled a rapid, non-destructive assessment of the inorganic constituents retained in the char after pyrolysis. XRF analysis indicates that the ash is rich in Fe, Ca, K, Al, and Si, suggesting the presence of mineral species capable of influencing thermochemical reaction pathways. These inorganic components can participate in secondary

Table 2 Elemental composition of the pyrolytic biochar

Elements		Value
Barium	Ba	529.38
Antimony (stibium)	Sb	23.01
Tin	Sn	90.74
Molybdenum	Mo	15.32
Niobium	Nb	6.95
Zirconium	Zr	177.18
Strontium	Sr	307.67
Rubidium	Rb	45.39
Bismuth	Bi	8.78
Arsenic	As	13.59
Lead	Pb	165.22
Zinc	Zn	2075
Copper	Cu	884.25
Iron	Fe	61 118.36
Manganese	Mn	409.24
Chromium	Cr	297.93
Vanadium	V	137.04
Titanium	Ti	5132.75
Calcium	Ca	58 158.83
Potassium	K	9480.56
Aluminium	Al	19 611.1
Phosphorus	P	20 043.3
Silicon	Si	78 152.92
Chlorine	Cl	764.58
Sulphur	S	8849.71

reactions by providing catalytically active sites that promote the breakdown of intermediate products formed during conversion. In particular, alkali and alkaline earth metals such as K and Ca are associated with enhanced cracking of higher hydrocarbons and increased char reactivity, which can shift product distributions toward lighter gaseous species. Iron-containing phases may further support these secondary reactions by facilitating the decomposition of oxygenated and hydrocarbon intermediates, thereby promoting hydrogen formation and influencing the H_2/CO ratio. In contrast, Al- and Si-rich phases are comparatively inert and primarily contribute to structural stabilisation within the ash matrix. Overall, the mineral composition of the ash appears to promote secondary conversion reactions that favour hydrogen formation, while not functioning as a dedicated catalyst system. These findings provide valuable information regarding the mineral retention and possible enrichment during pyrolysis, supporting further evaluation of the char's potential applications in areas such as environmental remediation, catalysis, or soil conditioning.

2.2 Microplastic extraction

The process for preparing samples of biochar and dried sludge microplastic samples were identical. 10 g of each sample were weighed and then sieved through a 2000 μm sieve to remove larger debris; the larger MPs could be easily identified and removed from the sieve. The fine particles were then treated with 20 mL of 30 v/v% H_2O_2 in a 50 °C water bath to remove organic matter. Additional hydrogen peroxide (H_2O_2) was added if the organic matter was still visible or if the reaction had not completed. Saturated sodium chloride (NaCl) solution (1.2 g mL^{-1}) was added and left overnight to separate by difference in density. The top aqueous layer was extracted using a syringe and vacuum filtered through Whatman Grade 1 filter paper (pore size of 11 μm) to capture the MPs on filter paper for analysis. The filtrate was then refiltered as this has shown to improve the retention of MPs. Finally, the filter papers were oven dried and stored in glass Petri dishes for microscopic analysis. All procedures were carried out in a fume hood to reduce airborne contamination.

It is important to note that the method evolved significantly as the process was developed. A more efficient aqueous layer isolation technique from the density separated sample was attempted *via* a separating funnel, however the clay sediment in the sludge blocked the stopcock. It is also important to control the rate of H_2O_2 addition as it was found that a fast reaction, if mixed quickly, resulted in a gritty and aerated sample, which took longer to settle during the density separation phase.

2.3 Identification and quantification

The identification method in this study was primarily based on optical microscopy. For optical microscopy, the limit of detection (LOD) was defined as the minimum number of microplastic particles that could be unambiguously distinguished from the sludge matrix under the applied imaging conditions. The limit of quantification (LOQ) was defined as the lowest particle count that could be consistently identified and enumerated with acceptable repeatability across replicate measurements. Based on procedural blanks and repeated observations, the practical LOD corresponded to one confirmed microplastic particle per analysed sample, while the LOQ was defined as the minimum count at which counting uncertainty was sufficiently reduced to enable reliable quantification.

Prior to visual analysis, samples of easily mistakeable organic material were analysed to avoid misidentification of MPs. Key identifiers to identify MPs included hollow tubular structures, splintered fibre tips, ridges, and symmetrical shapes. Salt crystals also posed an identification issue, as copper crystals appeared green/blue, and orange/brown crystals were also common. However, their simple geometric features helped differentiate them from MPs and excluded them from the count.

On each sample, 4–5 5 × 5 mm areas were examined for MPs $<$ 50 μm while 3–5 20 × 20 mm areas were inspected for MPs $>$ 50 μm. The type of MP (fragment, fibre, bead, or glitter) was noted, along with its colour, longest axis length and MP area if applicable. Blanks were also analysed to gauge the extent of MP contamination. Once the MP count was concluded, the debris on the filter paper was analysed using FTIR spectroscopy to determine the chemical composition of the MPs. For FTIR analysis, the LOD was defined as the smallest MP particle capable of producing an infrared spectrum with sufficient signal-to-noise ratio to allow polymer identification. The limit of quantification LOQ was defined as the minimum spectral quality at which polymer composition could be consistently and confidently identified based on library matching criteria.

2.4 Quality control

There was a high risk of sample contamination due to the presence of MP debris in all environments. Fibres from synthetic clothing and particles from plastic laboratory equipment were the greatest risk, hence standard operating procedures were always followed.[43] The following precautions were taken:

- Only distilled water was for process such as filtering and equipment cleaning.
- Use of glass or metal equipment to minimize plastic contamination.
- No synthetics clothing was worn in the laboratory. A 100% cotton, white lab coat was always worn.
- Covering open samples with aluminium foil.

Blank tests were also conducted through the pre-treatment steps and then analysed for MPs, to be used as negative controls. The use of blanks was very important to provide a baseline contamination value that can be subtracted from MPs counts in all the biochar and sludge samples. Previous studies provide blank MP concentrations ranging from 0 to 36 particles per blank.[44] Blanks are extremely important for the biochar samples where the expected MP count is very small, and MP contamination could make up a large percentage of the present MPs. Studies also recommend MP detection work to only be conducted in a room with limited access and controlled air flow *via* means of a laminar flow hood.[45] This study relies on the

sterility of the working environment to offset the uncontrolled air environment.

3. Results and discussion

3.1 Pyrolyser performance and energy recovery

3.1.1 Syngas analysis. The effect of auger speed on the composition of syngas generated from the pyrolysis of sewage sludge at 800 °C is illustrated in Fig. 2. The observed gas products include hydrogen (H_2), carbon monoxide (CO), carbon dioxide (CO_2), methane (CH_4), ethylene (C_2H_4), and light hydrocarbons in aggregate form (C_nH_m). Among these, hydrogen consistently exhibits the highest volumetric share across all operating conditions, followed by CO and CH_4. It is evident that variations in auger speed significantly influence the relative concentration of these gaseous components.

At an auger speed of 3 rpm (rotations per minute), which corresponds to the longest residence time within the pyrolysis reactor, the highest yield of H_2 (~41%) was recorded. This enhanced hydrogen production can be attributed to prolonged exposure of volatile compounds to elevated temperatures, promoting secondary reactions such as tar cracking and the water-gas shift reaction. Additionally, higher levels of CO (~23%) at this speed indicate that carbon–oxygen gas–solid interactions, such as the Boudouard reaction ($C + CO_2 \rightarrow 2CO$), were more dominant under extended residence times. CH_4 and CO_2 levels were comparatively lower at 3 rpm, suggesting that primary pyrolysis products had sufficient time to undergo further thermal decomposition and reforming. As the auger speed increased to 5 rpm, a moderate decline in H_2 concentration (~37%) was observed, accompanied by a slight rise in CH_4 and CO_2. This suggests a partial suppression of secondary gas-phase reactions due to reduced residence time. Nevertheless, the intermediate auger speed appears to offer a balance between adequate heating and moderate throughput, yielding syngas of reasonable quality. At the highest auger speed of 10 rpm, the residence time was shortest, leading to a noticeable reduction in H_2 content (~34%) and CO (~18%). In contrast, CH_4 and CO_2 concentrations reached their peak values under this condition. These trends indicate that at higher auger speeds, the pyrolysis process is dominated by primary devolatilization reactions, with limited time for secondary cracking or reforming. As a result, more light hydrocarbons and unconverted volatiles remain in the syngas, reducing its calorific value and hydrogen content.

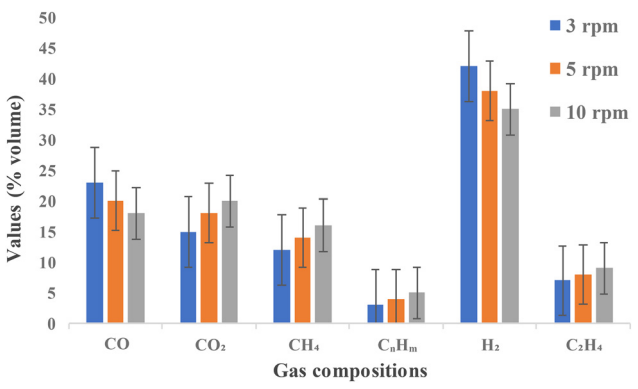

Fig. 2 Syngas profiles under varying conditions.

3.1.2 Gasification rate and heating value analysis. The effect of auger speed on sludge gasification was evaluated by varying the auger rotation from 10 to 3 rpm, and the resulting product distributions and syngas properties are summarised in Table 3. As the auger speed decreased, the fraction of sludge converted to gas increased from 58.1 wt% at 10 rpm to 65.1 wt% at 3 rpm, while the corresponding char yield decreased from 41.9 wt% to 34.9 wt%. This trend is accompanied by a reduction in volumetric gas flow rate from 5.4 L min^{-1} at the highest speed to 1.8 L min^{-1} at the lowest, reflecting the increased residence time and more complete conversion of the feedstock. LHV of the produced syngas showed a slight increase with decreasing auger speed, rising from 17.01 MJ m^{-3} at 10 rpm to 17.42 MJ m^{-3} at 3 rpm, indicating that slower auger operation favours the formation of a more energy-dense, hydrogen-rich gas. Overall, these results highlight the influence of auger speed on both the gasification efficiency and the energy content of the syngas, demonstrating that reduced auger rotation enhances hydrogen-laden syngas production while decreasing char generation.

3.2 Indicative techno-economic considerations

An initial assessment of energy performance and economic feasibility is presented using indicative metrics derived from the experimental data. The specific energy for sludge dry using domestic electrical tumble dryer is estimated at 6.3 kWh kg^{-1} water removed, while a simplified net energy balance shows that the chemical energy of the produced syngas (~14.2 MJ kg^{-1} dry sludge) covers a substantial fraction of the main process energy demands. Indicative operating costs are assumed at 1.89 £ per kg for drying sludge and capital costs at 6000 £ for a pilot-scale pyrolyser unit with a capacity of 1 kg h^{-1}. Hydrogen productivity is reported as 0.12 N m^3 H_2 per kg dry sludge. These metrics provide an initial framework for assessing energy performance and economic feasibility, while a detailed technoeconomic assessment is identified as an important area for future work, particularly in relation to scale-up and deployment.

3.3 Microplastic count

Using an optical microscope, plastics were found in all investigated sludge samples from wastewater treatment plants. Initial counts showed an average of 89.0 MP per gram of dried sludge. However, by examining the blank test, it was found that

Table 3 Pyrolyser performance and syngas properties at different auger speeds

Auger speed (rpm)	Gasified sludge (wt%)	Char (wt%)	Volumetric flow rate (L min^{-1})	LHV (MJ m^{-3})
10	58.1	41.9	5.4	17.01
5	61.9	38.2	2.7	17.27
3	65.1	34.9	1.8	17.42

approximately 17.4 of these MPs were contaminants collected during the pre-treatment process. After adjusting for this contamination, the corrected value was 71.6 MP per g of dried sludge. Miss-identification and overestimation are other sources of error that were not accounted for in this study.

FTIR spectroscopy can be used to test individual MPs to confirm their plastic composition. However, this study could not implement this due to the time required to isolate and test individual MPs. Hence, misidentification parameters from similar studies were used. Previous studies state that from micro-FTIR/Raman spectroscopy, roughly 75% ± 10% of suspected MPs are confirmed.[24] By applying this percentage to the count from this study, a total of 53.7 ± 7.2 MPs were identified in the sludge. 1 kg of wet sludge (WS) produced on average 425 g of dried material, hence the WS concentration can be estimated to be 22 823 ± 3060 MP per kg. Within the 3.5 million tonnes of sewage used as fertilizer in the UK in 2020, this would account for roughly 79.9×10^{12} MPs.[46]

MPs were also identified in the biochar samples. However, it was observed that on average only 16.2 MP per g of biochar which is very close to the average contamination level. Furthermore, most of the MPs observed were deduced to be mistaken metal beads or vividly coloured MPs, which would not survive in residue heated to +800 °C. Hence it was concluded that no original MPs remained in the biochar. The high temperature pyrolysis implemented in this study, which heated the feedstock to over 500 °C above the highest melting point of plastics. Hence, polymer decomposition is guaranteed to remove most MPs. Further studies could reveal to what extent MPs combine with other content (organic and metallic) in the sludge during heating to form new polymers. Fig. 3 and 4 depicts the MPs from sludge and contamination in char respectively. The blank test revealed that 83% of contaminants were fibres with the remaining 17% being fragments. The colours of these contaminants were evenly split between blue, black, and colourless.

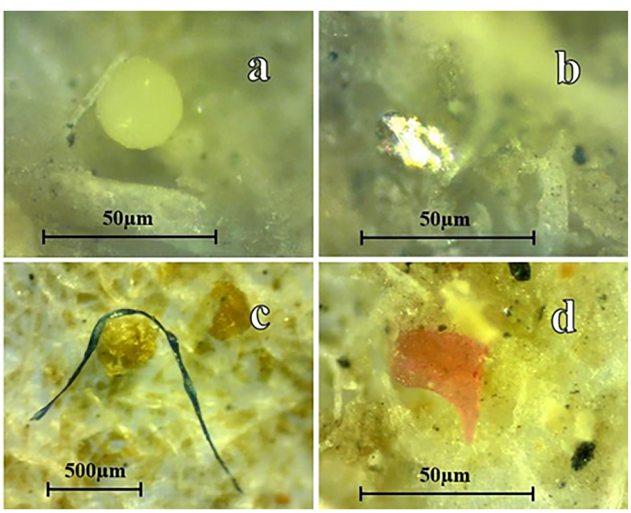

Fig. 3 Examples of MPs from sludge: microbead (a), glitter (b), fibre (c) and fragment (d).

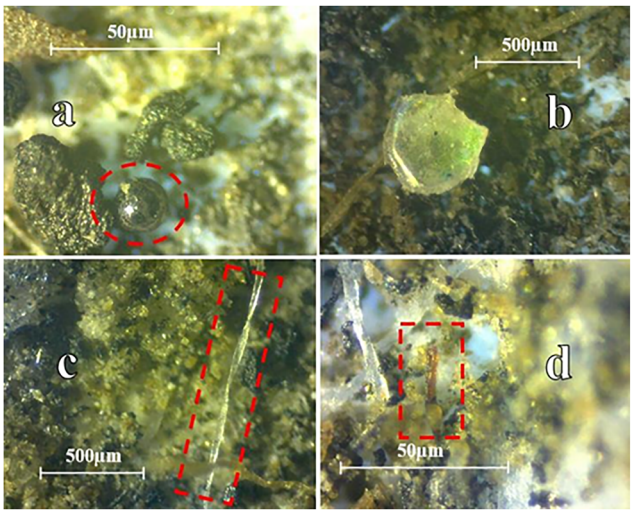

Fig. 4 Examples of contamination in biochar: metal bead (a) and contaminated MP fragment (b) and fibres (c) and (d).

3.3.1 Characterisation by type. MPs were characterised by shape during the visual identification process as depicted in Fig. 5. Firstly, in the dried sludge, fragments were most common (~46.2%) closely followed by fibres (~41.9%), then beads (~10.3%) and glitter (~1.7%). Some studies also characterise foams, however, none were identified in this study. Additionally, other studies also often find anomalies from nearby industries, distorting the type of MP distribution.[47] However, due to the very large variety of colours and sizes examined later, this was not the case in this study.

In the biochar primary count, 40% of the potential MPs were beads, followed by a joint 30% for both fibres and fragments. However, as previously mentioned, it was assumed that the beads were likely composed of metal, whilst the fragments and fibres were considered probable contaminants.

3.3.2 Characterisation by size. As depicted in Fig. 6, the size of visually identified MPs in the dried sludge ranged from 2.04 µm to +2000 µm with an average size of 767.12 µm. 76.9% of the identified MPs were classified as small microplastics (<1 mm). It is important to note that MPs > 2000 µm could not be measured precisely due to limitations of the microscopic camera.

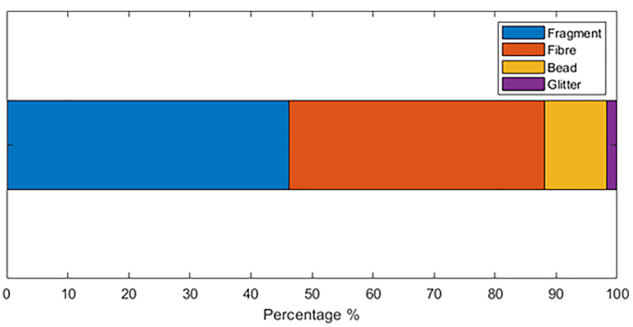

Fig. 5 Characterisation of MP in dried sludge by type.

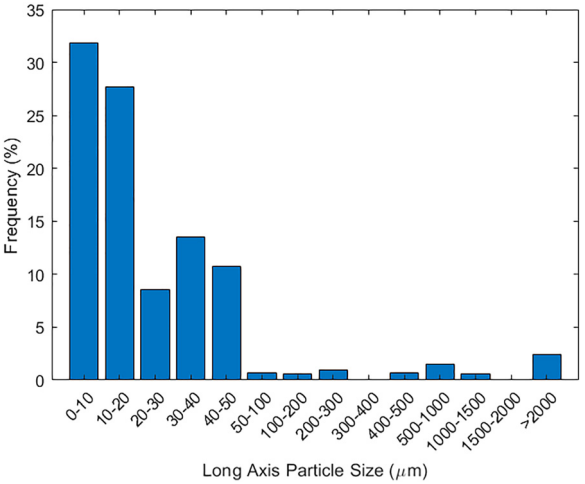

Fig. 6 Size distribution of MPs in sludge.

Within the scope of this study, it was easier to identify MPs > 2000 μm, which presented some bias in their quantification. On the other hand, MPs < 10 μm were difficult to identify as they permeated the filter paper to different depths, in many cases making them unobservable. Thus, the limitation in pore size (11 μm) meant that the retention of MPs < 10 μm was not 100% and so the quantity recorded was an underestimate. Further complications arose from the filter paper, as to an untrained eye filter fibre could easily be mistaken for MP fibres.

83% of the identified microbeads had an exact, two significant figure size with 25% being exactly 200 μm in diameter. This is comparable to the average size of microbeads identified in cosmetic products.[48] As shown in Table 4, the microbead and glitter concentrations represented only those MPs that could be confirmed as primary MPs. This accounted for only 12.0% of the total identified MPs. Despite this low concentration, it was nevertheless surprising to discover microbeads, as the UK banned their use in the manufacturing of cosmetic and personal care products in 2018.

The observable area of each MP was recorded for fragments, beads and glitter. Fragments had the largest average area (43 846 μm^2), followed by microbeads (15 784 μm^2) and glitter (4278 μm^2), as Tabulated in Table 5. Manufactured to specific sizes, the smaller distribution of particle area for both beads and glitter reflected their primary MP source. The largest distribution of area was measured for fragments which demonstrated their secondary source, due to the more random degradation of larger plastics.

3.3.3 Characterisation by colour. The classification of MP colours is shown in Table 6. Blue MPs were the most prevalent (26.5%), followed closely by clear MPs (24.8%). Colour is a subjective parameter with no defining trends, however, by identifying 12 colours, a range of sources of MPs were illustrated. It is important to recognise that during the H_2O_2 organic removal process, some plastics appeared to become bleached. This increased the proportion of colourless MPs identified, especially with respect to fibres which often showed partial/incomplete bleaching. As mentioned previously, the filter paper could also appear as colourless fibres within the samples. However, with both the filter paper and bleached organic material, awareness of cellulose's structural characteristics prevented misidentification of these fibres as MPs.

Table 4 Average size of MP types in sludge

Average particle size (μm)			
Fragment	Fibre	Bead	Glitter
144.63	1643.20	107.32	69.08

Table 5 Area of MPs

	Particle area (μm^2)		
	Fragment	Bead	Glitter
Average	43 846	15 784	4278
Maximum	929 298	5929	8344
Minimum	3.3	78.5	212.9

Table 6 Colour distribution of MPs identified in sludge

Overall %		Fragment	Fibre	Bead	Glitter
Blue	26.5%	71.0%	29.0%	0	0
Clear	24.8%	0	72.4%	27.6%	0
Black	12.8%	6.7%	93.3%	0	0
Red	12.8%	93.3%	6.7%	0	0
Green	10.3%	91.7%	8.3%	0	0
Orange	3.4%	75%	0	25%	0
White	2.6%	0	0	100%	0
Multi	1.7%	0	0	0	100%
Grey	1.7%	0	100%	0	0
Pink	1.7%	100%	0	0	0
Yellow	0.9%	100%	0	0	0
Purple	0.9%	0	100%	0	0

3.4 FT-IR analysis

Following visual identification, the loose debris from the filter paper was extracted and examined under an FT-IR spectrometer, as depicted in Fig. 7. Blank cellulose samples were tested alongside the sludge samples for comparison. By analysing the spectra of different plastics, it was found that the results from the sludge samples closely matched to those of polyethylene terephthalate (PET), the world's most widely manufactured plastic.[49] The blank samples had the large cellulose defining O–H peaks at 3330 cm^{-1}, which were not as prominent in the sludge samples.[50,51]

The absorption band observed in the 1650–1550 cm^{-1} region is attributed to C=C stretching vibrations, indicative of unsaturated and/or aromatic structures that are more commonly associated with microplastic materials than with cellulose.[52] The absorption band observed near 1700 cm^{-1} is attributed primarily to aromatic C=C stretching vibrations associated with the benzene rings in polyethylene terephthalate. Ester carbonyl (C=O) stretching typically appears at slightly higher wavenumbers (1715–1730 cm^{-1}), consistent with established FTIR literature for PET.[53,54] Finally, the C–O

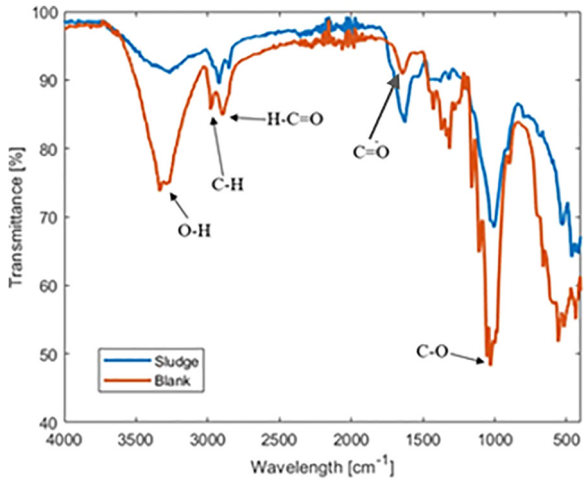

Fig. 7 FT-IR spectra comparison between blank and MP sample.

absorption band near 1050 cm^{-1} was noticeably weaker in the sludge sample, indicating a lower contribution from cellulose-related compounds and presence of plastic-derived material. At the same time, this feature cannot be attributed solely to microplastics, as similar C–O vibrations may also originate from residual organic matter, mineral-associated species, or products formed during thermal transformation.

3.5 Comparison with previous studies

Previous studies used micro-FT-IR to analyse individual MPs for their composition and to illustrate the distribution of polymer type.[14] These studies revealed that PET is the most abundant MP. However, they also quantified significant proportion of polypropene, polystyrene polyamide and others. Numerous studies have quantified the MP content of sludge. The results from this study (53.7 ± 7.2 MP per g dried sludge) compliment the results from similar research, which report values ranging from 50 to 200 MPs per g.[24] A few studies reveal values exceeding 500 MP per g,[22] however this is related to the specific use of micro-Raman spectroscopy and finer mesh sizes, which were not implemented in this study due to time and resource constraints. The level of contamination in this study was comparably high, at 17.4 MP per g. This can largely be attributed to the shared working environment. However, some studies do reveal more contamination level, up to 36 MP per g.[55]

Similar distributions of MP length are consistent with findings from MP analyses across various environment, from marine to clay sediments. As MP length decreases, their quantity increases, most significantly for particles smaller than <100 μm.[19,27] Similarly, the distribution of colours is highly comparable to other studies analysing MPs in a range of environments. This reflects similar sources of MPs worldwide and highlights the large domestic source. Finally, the distribution of MP particle types in this study also matched those from other studies. Previous studies reveal variability of microplastic shapes, even when samples are collected only several kilometres apart.[47] This variability can be attributed to the type of industries and urban developments that feed certain MP sinks. Whereas on a global scale, contrasting results can be likely due to varying pollution levels alongside MP manufacturing laws and regulations.

4. Conclusion

This study highlights the potential of pyrolysis as a dual-function strategy for hydrogen-rich syngas generation and microplastic removal from sewage sludge. Experiments conducted at 800 °C showed that reduced auger speeds significantly enhanced hydrogen production, achieving concentrations up to 41 vol% due to prolonged residence time and improved secondary reforming reactions.

A straightforward and resource-efficient method was applied to quantify MPs in the sludge feedstock and the resulting biochar. The feedstock contained an average of 53.7 ± 7.2 MPs per g, characterized by type, shape, size, and colour. FTIR analysis confirmed the likely presence of PET-based plastics in the sludge, though any remaining particles in the biochar were visually distinct and easily identified as non-MP artefacts.

Given the temporal variability of MP concentrations in wastewater treatment plant outputs linked to seasonal and environmental changes, future work should focus on long-term monitoring, process optimization and also techno economic assessment. These findings contribute to the development of decentralized waste-to-hydrogen technologies while addressing growing concerns over microplastic pollution.

Declaration of generative AI in scientific writing

During the preparation of this work the authors used ChatGPT to improve the language. After using this tool/service, the authors reviewed and edited the content as needed and take full responsibility for the content of the published article.

Conflicts of interest

There are no conflicts to declare.

Data availability

Data for this article are available in Durham University Research Data Repository at https://doi.org/10.15128/r2k0698758q.

Acknowledgements

This research was delivered with financial support from the Innovate UK Project for a project entitled "Development of a sewage sludge waste containing microplastics pyrolysis plant for sustainable hydrogen, syngas and high-quality pyrolytic char production (PyroPlus)", Project no. 10032591. We gratefully acknowledge the technical assistance of Mr Jonathan Heslop, Senior Technician at Durham University, and the

continued collaboration and expertise provided by Dr Rehman Rafiq and Dr Arsalan Ashraf from Hybrid Gasification Ltd, whose contributions were instrumental to the successful execution of this study.

References

1 Department for Energy Security and Net Zero, UK Parliament, 2023, https://assets.publishing.service.gov.uk/media/64dc8d3960d123000d32c602/biomass-strategy-2023.pdf.
2 H. G. Castellanos, Y. Aryanfar, A. Keçebaş, M. E. H. Assad, S. Islam, Q. N. Naveed and A. Lasisi, *J. Water Process Eng.*, 2024, 104987.
3 H. Sun, D. Feng, S. Sun, Y. Zhao, L. Zhang, G. Chang, Q. Guo, J. Wu and Y. Qin, *J. Anal. Appl. Pyrolysis*, 2021, **156**, 105128.
4 Y. W. Cheah, R. Intakul, M. A. Salam, J. Sebastian, P. H. Ho, P. Arora, O. Öhrman, D. Creaser and L. Olsson, *Chem. Eng. J.*, 2023, 146056.
5 F. Beik, L. Williams, T. Brown and S. T. Wagland, *Energy Convers. Manage.*, 2023, **277**, 116627.
6 X. Pan, Y. Wu, T. Li, G. Lan, J. Shen, Y. Yu, P. Xue, D. Chen, M. Wang and C. Fu, *Renew. Energy*, 2023, **215**, 118946.
7 A. Mulchandani and P. Westerhoff, *Bioresour. Technol.*, 2016, **215**, 215–226.
8 K. Fijalkowski, A. Rorat, A. Grobelak and M. J. Kacprzak, *J. Environ. Manage.*, 2017, **203**, 1126–1136.
9 ECHA, Microplastics, https://echa.europa.eu/hot topics/microplastics.
10 NOAA, What are microplastics? https://oceanservice.noaa.gov/facts/microplastics.html.
11 C. M. Rochman, *Oceanography*, 2020, **33**, 60–70.
12 M. Bao, Q. Huang, Z. Lu, F. Collard, M. Cai, P. Huang, Y. Yu, S. Cheng, L. An, A. Wold and G. W. Gabrielsen, *Environ. Sci. Pollut. Res.*, 2022, **29**, 56525–56534.
13 H. Lai, X. Liu and M. Qu, *Nanomaterials*, 2022, **12**, 1298.
14 D. Harley-Nyang, F. A. Memon, N. Jones and T. Galloway, *Sci. Total Environ.*, 2022, **823**, 153735.
15 W. Liu, J. Zhang, H. Liu, X. Guo, X. Zhang, X. Yao, Z. Cao and T. Zhang, *Environ. Int.*, 2021, **146**, 106277.
16 S. Ziajahromi, P. A. Neale and F. D. L. Leusch, *Water Sci. Technol.*, 2016, **74**, 2253–2269.
17 C. G. Avio, S. Gorbi, M. Milan, M. Benedetti, D. Fattorini, G. D'Errico, M. Pauletto, L. Bargelloni and F. Regoli, *Environ. Pollut.*, 2015, **198**, 211–222.
18 Y. Dong, M. Gao, W. Qiu and Z. Song, *Ecotoxicol. Environ. Safe.*, 2021, 111899.
19 S. M. Mintenig, I. Int-Veen, M. G. J. Löder, S. Primpke and G. Gerdts, *Water Res.*, 2017, **108**, 365–372.
20 J. N. Möller, M. G. J. Löder and C. Laforsch, *Environ. Sci. Technol.*, 2020, **54**, 2078–2090.
21 European Biochar Industry Consortium, Sewage Sludge as feedstock for pyrolysis to be included in the scope of the EU Fertilizing Products Regulation, https://cdn.prod.website-files.com/66d0896fda2fb8a0d53224d6/675946c2c8be0c8736b90a75_20230131_EBI_Sewage_Sludge_Position_Paper_final.pdf.
22 B. J. Ni, Z. R. Zhu, W. H. Li, X. Yan, W. Wei, Q. Xu, Z. Xia, X. Dai and J. Sun, *Environ. Sci. Technol. Lett.*, 2020, **7**, 961–967.
23 K. V. Shivaprasad, J. Heslop, D. Roy, A. Malik, Y. Wang, A. P. Roskilly and H. Bao, *Process Saf. Environ. Prot.*, 2024, **187**, 270–278.
24 X. Li, L. Chen, Q. Mei, B. Dong, X. Dai, G. Ding and E. Y. Zeng, *Water Res.*, 2018, **142**, 75–85.
25 D. Friot and J. Boucher, *Primary microplastics in the oceans: A global evaluation of sources*, IUCN Gland, Switzerland, 2017.
26 A. A. Koelmans, A. Bakir, G. A. Burton and C. R. Janssen, *Environ. Sci. Technol.*, 2016, **50**, 3315–3326.
27 D. Neves, P. Sobral, J. L. Ferreira and T. Pereira, *Mar. Pollut. Bull.*, 2015, **101**, 119–126.
28 Marine Conservation Society, Sewage sludge: Why we need to stop pollution at source, https://www.mcsuk.org/news/sewage-sludge-why-we-must-stop-pollution-at-source/.
29 C. Dowler and Z. Boren, *Unearthed*, Greepeace, 2020, pp. 1–10.
30 S. J. Cusworth, W. J. Davies, M. R. McAinsh and C. J. Stevens, *Plants People Planet*, 2024, **6**, 304–314.
31 F. Büks and M. Kaupenjohann, *Soil*, 2020, **6**, 649–662.
32 E. Dümichen, P. Eisentraut, C. G. Bannick, A. K. Barthel, R. Senz and U. Braun, *Chemosphere*, 2017, **174**, 572–584.
33 S. Fuller and A. Gautam, *Environ. Sci. Technol.*, 2016, **50**, 5774–5780.
34 D. Liu, L. Zhang, B. Zhang, Y. Bai, L. Zhao, J. Gao, C. Xu, H. Liu and X. Liu, *Chem. Eng. Sci.*, 2022, **257**, 117718.
35 S. Zhang, X. Yang, H. Gertsen, P. Peters, T. Salánki and V. Geissen, *Sci. Total Environ.*, 2018, **616–617**, 1056–1065.
36 K. A. V. Zubris and B. K. Richards, *Environ. Pollut.*, 2005, **138**, 201–211.
37 M. Sajjad, Q. Huang, S. Khan, M. A. Khan, Y. Liu, J. Wang, F. Lian, Q. Wang and G. Guo, *Environ. Technol. Innovation*, 2022, **27**, 102408.
38 M. Fischer and B. M. Scholz-Böttcher, *Environ. Sci. Technol.*, 2017, **51**, 5052–5060.
39 M. Majewsky, H. Bitter, E. Eiche and H. Horn, *Sci. Total Environ.*, 2016, **568**, 507–511.
40 M. Vasudeva, A. K. Warrier, V. B. Kartha and V. K. Unnikrishnan, *TrAC, Trends Anal. Chem.*, 2025, **183**, 118111.
41 J. L. Xu, K. V. Thomas, Z. Luo and A. A. Gowen, *TrAC, Trends Anal. Chem.*, 2019, **119**, 115629.
42 L. Cabernard, L. Roscher, C. Lorenz, G. Gerdts and S. Primpke, *Environ. Sci. Technol.*, 2018, **52**, 13279–13288.
43 J. C. Prata, V. Reis, J. P. da Costa, C. Mouneyrac, A. C. Duarte and T. Rocha-Santos, *J. Hazard. Mater.*, 2021, **403**, 123660.
44 Y. Fan, K. Zheng, Z. Zhu, G. Chen and X. Peng, *Environ. Pollut.*, 2019, **251**, 862–870.
45 C. Scopetani, D. Chelazzi, A. Cincinelli and M. Esterhuizen-Londt, *Environ. Monit. Assess.*, 2019, **191**, 652.
46 Assured Biosolids, Microplastics position statement Nov 2023, https://assuredbiosolids.co.uk/wp-content/uploads/2023/11/Microplastics-Position-Statement-Nov-2023.pdf.

47 T. Jennifer, Durham E-Theses. https://etheses.dur.ac.uk/15092/.
48 P. Möhlenkamp, A. Purser and L. Thomsen, *Elementa*, 2018, **6**, 61.
49 C. Trilokesh and K. Babu Uppuluri, *Sci. Rep.*, 2019, **9**, 16709.
50 B. Chen, M. S. Wijesinghe, A. Grimaud and M. M. Waegele, *J. Phys. Chem. Lett.*, 2025, **16**, 1779–1786.
51 N. Mohandas, T. N. Narayanan and A. Cuesta, *ACS Catal.*, 2023, **13**, 8384–8393.
52 H. A. Ezzat, N. M. El Sayed, D. Shehata, H. Elhaes, A. Ibrahim, H. Kalil, M. A. Ibrahim, M. M. Yousef, I. S. Yahia, H. Y. Zahran and I. Gomaa, *Sci. Rep.*, 2024, **14**, 1–13.
53 J. Coates, *Encyclopedia of Analytical Chemistry*, Wileys, Chichester, 2000, pp. 10815–10837.
54 G. Socrates, *Infrared and Raman Characteristic Group Frequencies: Tables and Charts*, Wiley, 3rd edn, 2004.
55 S. Frei, S. Piehl, B. S. Gilfedder, M. G. J. Löder, J. Krutzke, L. Wilhelm and C. Laforsch, *Sci. Rep.*, 2019, **9**, 15256.